

Electronic conductivity in Berlin green and Prussian blue

Daniel M. Pajerowski, Takeshi Watanabe, Takashi Yamamoto, and Yasuaki Einaga

Department of Chemistry, Keio University, 3-14-1 Hiyoshi, Yokohama 223-8522, Japan

(Received 28 September 2010; revised manuscript received 18 January 2011; published 18 April 2011)

We report the temperature dependent (100–300 K) conductivity of Berlin green and Prussian blue powders. The method of electronic conduction in vacuum dried Berlin green is identified as hopping of localized electrons and vacuum dried Prussian blue is reaffirmed as an insulator. The assignment of the conduction mechanism is based upon fits to the experimental data, and the different conductivities of the two samples can be understood in terms of both molecular and simple crystalline energy levels of the solids.

DOI: [10.1103/PhysRevB.83.153202](https://doi.org/10.1103/PhysRevB.83.153202)

PACS number(s): 72.20.-i, 75.50.Xx, 84.37.+q

Prussian blue, $\text{Fe}_4^{3+}[\text{Fe}^{2+}(\text{CN})_6]_3 \cdot x\text{H}_2\text{O}$, is the prototypical hexacyanometallate network,^{1,2} and has served as a model system for increasing understanding of materials in the solid state as the science has progressed over time.³ Prussian blue (PB) crystallizes in a cubic structure, in which cyanide ligands octahedrally coordinate the metal ions, and metal vacancies and interstitial cations are essential for local charge balance of the structure.¹ More than only bolstering fundamental knowledge, the study of Prussian blue analogs (PBAs) has seen a renaissance as materials possessing a variety of functional properties have been reported.⁴ While the magnetic properties of PBAs have been studied in great detail,⁴ the electronic conducting properties may yet hold some surprises.

The electric conductivity of PB and analogous compounds has been under investigation in some form since at least 1928.⁵ This field was further advanced with electrochemical studies of PB modified electrodes, which have the advantage of facile study of oxidized (yellow) and reduced (white) forms.⁶ However, electrochemically prepared films are unstable when dried, with an inevitable return to the PB form, and wet conduction is dominated by ionic effects in addition to wet films being electrochemically active.^{6–8} In spite of these difficulties, both electrochemical and solid-state studies have confirmed striking differences between the conductivity of ferriferrocyanide (blue), ferriferrocyanide (yellow), and ferroferrocyanide (white); while vacuum dried PB acts as an insulator, the oxidized (yellow) and reduced (white) forms display semiconducting properties.^{9,10} Although different mechanisms have been speculated, a microscopic understanding of these changes in conductivity has not yet been confirmed.

Recently, experimental and theoretical reports relevant to understanding the conduction of PBAs have surfaced. A sodium cobalt hexacyanoferrate PBA showed a nonexponential relationship between resistance and temperature, as well as conductance switching as charge transferred between Co and Fe during thermal cycling.¹¹ Also, a vanadium hexacyanochromate PBA showed a modification of the conductivity during cooling through the magnetic ordering transition.¹² Detailed density-functional theory based studies of the electronic structure of PB show it to have a wide band gap between the valence and conduction bands.¹³ In addition, similar methods have predicted a half-metallic behavior for oxidatively and reductively doped PB, wherein the majority spin is insulating and the minority spin has conducting states available near the

Fermi energy.¹⁴ These predictions provided motivation for the current study, to probe the viability of hexacyanometallate networks for potential use in spintronic devices.

In this Brief Report, we investigate the conducting properties of a partially oxidized PB material, which is often called Berlin green (BG), over a wide temperature range and under vacuum. Berlin green was chosen because it is chemically stable for longer than the time scale of the experiment (at least more than one week), and it can be approximated as oxidatively doped PB. The effect of the change in oxidation from PB to BG on the electron conductivity is assessed in terms of the electronic structure.

Prussian blue was prepared using slow addition via separatory funnel of 100 ml, 100 mM $\text{K}_3\text{Fe}(\text{CN})_6$ aqueous solution to 100 ml, 100 mM FeCl_2 aqueous solution. Berlin green was prepared using slow addition via separatory funnel of 100 ml, 100 mM $\text{K}_3\text{Fe}(\text{CN})_6$ aqueous solution to 80 °C, 200 ml, 100 mM FeCl_3 aqueous solution. Precipitates were obtained via centrifugation at 5000 rpm for 20 min, and were subsequently washed with deionized (DI) water and dried under vacuum. Powder x-ray-diffraction (XRD) was performed on a Bruker Advanced X-ray Solutions D8 ADVANCE x-ray diffractometer with a $\text{Cu } K_\alpha$ source ($\lambda = 1.5418 \text{ \AA}$) and the samples showed peaks characteristic of the simple cubic $Fm\bar{3}m$ (No. 225) space group, Fig. 1(a). The PB lattice constant of 10.16 \AA is consistent with previous reports,¹ as is the BG lattice constant of 10.21 \AA .¹⁵ Infrared (IR) spectroscopy was performed on a JASCO FT-IR 660Plus spectrometer using vacuum dried slurry deposited on CaF_2 slides. Cyanide stretching peaks are clearly visible in the spectra for both samples, with PB having only one peak at 2070 cm^{-1} , associated with an $\text{Fe}^{2+}\text{-CN-Fe}^{3+}$ moiety, and BG having two peaks at 2080 and 2168 cm^{-1} [Fig. 1(b)], associated with $\text{Fe}^{2+}\text{-CN-Fe}^{3+}$ and $\text{Fe}^{3+}\text{-CN-Fe}^{3+}$ regions, respectively.¹⁶ The reported ratio of extinction coefficients for the mixed valence and oxidized cyanide stretches of approximately 3:1 can be used to extract an $\text{Fe}^{2+}\text{-CN-Fe}^{3+}:\text{Fe}^{3+}\text{-CN-Fe}^{3+}$ ratio of 1:1.2 for the BG samples studied in this Brief Report.¹⁶ X-ray photoelectron spectroscopy (XPS) was performed on a JEOL JPS-9000MX spectrometer using vacuum dried samples deposited on glass slides and the relative composition of K, N, and Fe in BG was measured. Combining the results of the IR and XPS measurements yields a chemical formula of $\text{Fe}_4^{3+}[\text{Fe}^{3+}(\text{CN})_6]_{1.9}[\text{Fe}^{2+}(\text{CN})_6]_{1.5} \cdot 3.6\text{H}_2\text{O}$ for BG, Table I. The water content in the reported formula is assumed to be

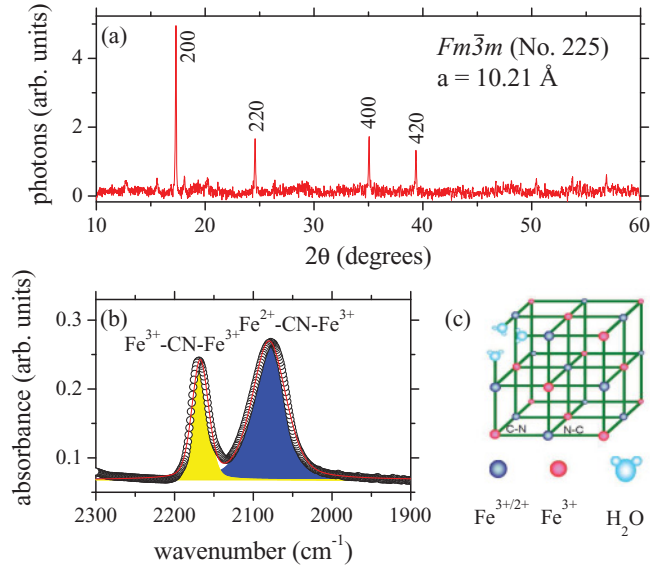


FIG. 1. (Color online) (a) An x-ray diffractogram of Berlin green with the prominent peaks, used to extract the lattice constant, indexed. (b) Infrared spectroscopy of Berlin green (○), fit (—) to a two-component model of $\text{Fe}^{3+}\text{-CN-Fe}^{3+}$ (yellow) and $\text{Fe}^{2+}\text{-CN-Fe}^{3+}$ (blue), with details in Table I. (c) A representation of the Berlin green structure.

only coordinated species because samples are measured under vacuum. The result of the sample characterization is a cubic structure with nitrogen coordinated Fe^{3+} ions and either Fe^{2+} or Fe^{3+} coordinated by carbon, with charge balance achieved by hexacyanoferrate vacancies; Fig. 1(c).

To measure the current as a function of applied voltage in the samples, BG and PB cells were prepared. Experimental cells consisted of a 1-cm \times 3-cm glass substrate with a layer of gold on the top with a small gap (≈ 100 μm) overfilled with the sample to be measured. Copper wires were attached to the gold layer using silver epoxy and connected to an Ivium CompactStat potentiostat/galvanostat. Temperature-dependent studies were performed using a duplex refrigerator equipped with a heater and thermocouple.

TABLE I. The proposed chemical formula of $\text{Fe}_4^{3+}[\text{Fe}^{3+}(\text{CN})_6]_{1.9}[\text{Fe}^{2+}(\text{CN})_6]_{1.5}\cdot 3.6\text{H}_2\text{O}$ for the Berlin green sample studied in this Brief Report is based on IR measurements, fit to a pseudo-Voigtian line $A(\mu \frac{2w}{4\pi(x-xc)^2+w^2} + (1-\mu)\sqrt{\frac{4\ln(2)}{\pi w^2}} e^{-4\ln(2)(x-xc)^2/w^2})$, and XPS measurements of the atomic percent concentrations.

IR				
Moiety	xc (cm^{-1})	A (arb. units)	w (cm^{-1})	μ
$\text{Fe}^{2+}\text{-CN-Fe}^{3+}$	2080	13.0	51.0	0.5
$\text{Fe}^{3+}\text{-CN-Fe}^{3+}$	2168	5.0	24.6	0.3
XPS				
	Fe	N	K	
% experiment	20.77	79.28	-0.05	
% proposed	26.62	73.38	0	

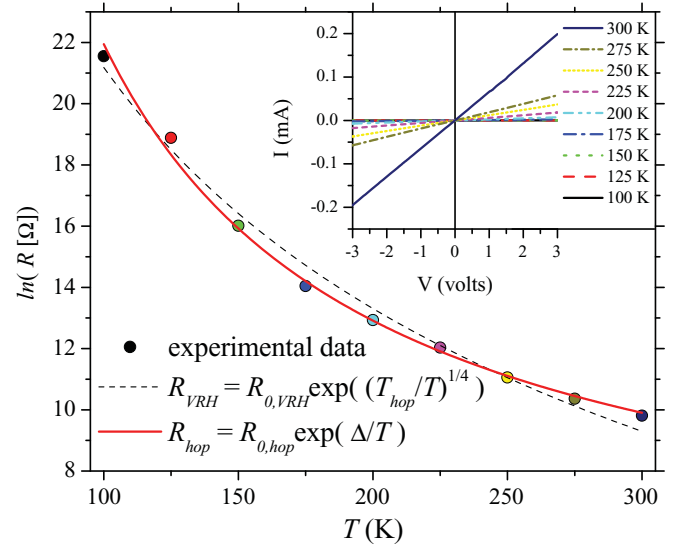


FIG. 2. (Color online) Temperature dependence of the resistance of Berlin green. The experimental data can be fit well to Mott's variable range hopping law with $\ln(R_{0,VRH}/\Omega) = -28.3 \pm 1.7$ and $T_{hop} = 156.5 \pm 6.1$ K or to nearest-neighbor hopping with $\ln(R_{0,hop}/\Omega) = 3.88 \pm 0.26$ and $\Delta = 0.155 \pm 0.003$ eV. (Inset) The individual I - V curves of Berlin green taken at different temperatures, which were fit to a line to extract the resistance. Below ≈ 100 K, no current could be resolved in the above voltage range.

The current-voltage curves for BG and PB were measured between -3 and 3 V at temperatures between 100 and 300 K. Berlin green showed ohmic resistance for all temperatures and voltages measured, with a nonexponential dependence of the resistance on temperature; Fig. 2. Prussian blue initially showed measurable, weak conduction, but after ≈ 30 min under vacuum did not show measurable current at all temperatures. This behavior is consistent with previous reports of the modification of the dielectric constant of PB due to interstitial water molecules.¹⁷ The issue of interstitial water molecules is important to control in order to avoid unknown sample variations, and in the vacuum conditions for these data, all interstitial solvent water has been pumped out of the sample, an assumption that is supported by the observed stabilization of insulating PB. Conversely, as an amplification of this point, if experiments are performed on PBAs at finite humidity, interstitial water molecules may provide a means for proton conduction in addition to providing extra crystal states for electronic conduction, making the task of discerning the nature of the charge movement through the lattice more convoluted.

The observed temperature dependence of resistance in BG is contrary to metallic conduction, however, various models of thermally activated conduction may be fit well to the data, such as $R_{SC} \propto e^{(E_{gap}/2k_B T)}$ for semiconductors¹⁸ or $R_{ion} \propto T e^{(E_a/k_B T)}$ for ionic conduction,¹² and physical reasoning must be invoked in concert with empirical facts to motivate the appropriate model. Thermally activated population of a conduction band is disconfirmed by the small gap ($E_{gap} \approx 0.3$ eV) that reproduces the observed temperature dependence, which is much smaller than the ≈ 2 eV predicted by density-functional theory,¹⁴ in addition to the inability of such a model to simply explain the difference in conduction

between PB and BG. Conduction via K^+ is ruled out by the absence of potassium in XPS experiments, as well as by the steady-state nature of the conduction, and no interstitial hydronium is possible due to the vacuum environment that has already been discussed. A physically motivated model is hopping of localized electrons that are otherwise expected to be metallic from band theory. Even in this regime, two distinct processes may occur, hopping to a neighboring state and variable range hopping to longer distances. Activation to a neighboring state results in a temperature-dependent resistivity

$$R_{hop} \propto e^{\Delta/k_B T} \quad \text{with} \quad \Delta = \frac{64}{9\pi D(E_F)\rho^3}, \quad (1)$$

while variable range hopping gives

$$R_{VRH} \propto e^{(T_{hop}/T)^{1/4}} \quad \text{with} \quad k_B T_{hop} = \Delta, \quad (2)$$

where R is resistance, T is temperature, $D(E_F)$ is the density of states (DOS) at the Fermi energy, k_B is Boltzmann's constant, and ρ characterizes the radial decay of the wave function (i.e., $\psi \propto e^{-r/\rho}$).¹⁹ The result of fitting to the variable range hopping model gives T_{hop} of the order of the measuring temperatures, Fig. 2, which does not meet the necessary condition for dominant variable range hopping that $T \ll T_{hop}$. Therefore the electrical conductivity in BG can be identified as activated hopping of localized electrons along nearest-neighbor sites.

The hopping of localized electrons through unoccupied crystal states is not surprising based upon what is known about the charge density in PBAs. Specifically, neutron-scattering and NMR measurements have shown that the unpaired electron density is strongly localized to the metal ion sites, with finite delocalization to the cyanide ligands.^{20,21} In addition, ioniclike wave functions have provided the basis for detailed understanding of the magnetism in PBAs.⁴

A semiquantitative description of the electronic structure of BG and PB is possible within the context of simple tight-binding theory. Calculations were performed using YAEHMOP and the standard parameter set was used.²² For crystalline calculations, the model lattice was generated using a $\text{Fe}_4[\text{Fe}(\text{CN})_6]_3\text{O}_6$ unit cell of length 10.2 Å, where the iron vacancy is coordinated by oxygen of solvent water. A mesh consisting of 40 symmetry-weighted k points in the irreducible part of the Brillouin zone was generated for space group $Fm\bar{3}m$ to compute DOS curves. Single-particle projected and total DOS show narrow bands that are characteristic of covalently bonded crystals with strongly ionic wave functions; see Fig. 3.²³ More sophisticated calculations show similar structure in the DOS.¹³ Molecular calculations were also performed for the $\text{Fe}(\text{CN})_6$ and $\text{Fe}(\text{NC})_4\text{O}_2$ units that approximate molecular building blocks of the lattice. Molecular calculations show a strong correspondence between molecular and crystalline states (Fig. 3). Both crystal and molecular energy levels show large gaps between the t_{2g} -like and e_g -like states that are near the Fermi energy. While more complicated theories are necessary for spin-dependent calculations,¹³ simpler tight-binding crystal calculations, and even tight-binding molecular calculations, can capture the qualitative features necessary to understand the unpolarized conducting properties in these ionic systems.

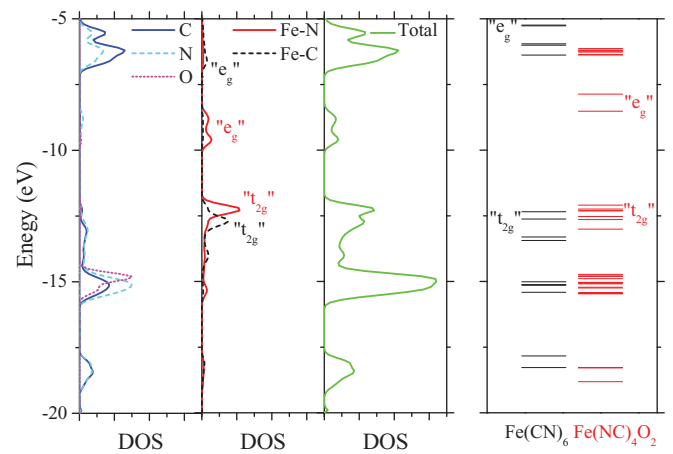


FIG. 3. (Color online) (left) Calculated $\text{Fe}_4[\text{Fe}(\text{CN})_6]_3\text{O}_6$ single-particle projected DOS for ligands, iron ions (Fe-C denoting carbon coordination and Fe-N denoting nitrogen and oxygen coordination), and all atoms. The contributions from 3d electrons to the iron ion DOS are labeled with either " t_{2g} " or " e_g " approximate symmetry. (right) Calculated energies for $\text{Fe}(\text{CN})_6$ and $\text{Fe}(\text{NC})_4\text{O}_2$. The contributions from 3d electrons are labeled with either t_{2g} or e_g approximate symmetry.

From the calculated energy levels, a simple scheme for the electron conduction can be proposed; see Fig. 4. For PB, the carbon coordinated Fe^{2+} ions have a full t_{2g} block, that prohibits conduction through those states. While e_g states are available, they are inaccessible for conduction due to an energy gap of the order of an electron volt, which is much greater than the thermal energy available at room temperature. Conversely, for BG, the existence of carbon coordinated Fe^{3+} sites yields unoccupied states in the t_{2g} block for both metal ions, providing a viable conduction channel at room temperature. However, as the electron density is strongly localized to the iron centers, a hopping process must occur for electrons to move through the lattice, with an effective energy barrier of the order of the thermal energy available at room temperature. Restated, the

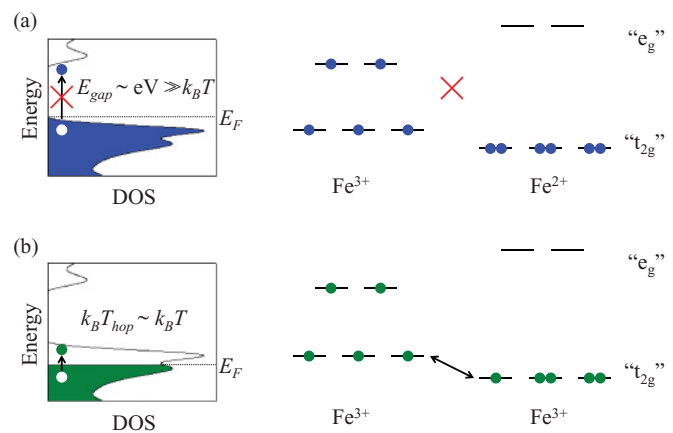


FIG. 4. (Color online) (a) Scheme of insulating behavior for PB due to a large energy gap E_{gap} between valence and conduction levels, in both crystal (left) and molecular (right) formulations. (b) Scheme of conducting behavior for BG due to thermally activated nearest-neighbor hopping, in both crystal (left) and molecular (right) formulations.

wide band-gap semiconductor PB may be oxidatively doped to decrease the Fermi energy and allow hopping conduction of localized electrons.

In conclusion, we have presented the temperature-dependent resistance of Prussian blue and Berlin green. The electron conduction mechanism in Berlin green has been identified as nearest-neighbor hopping conduction due to localized $3d$ electrons, and the conduction properties of Prussian blue can be categorized as a band insulator. As the important parameters of the current model are the radial diffusivity of the wave function and the density of states at the Fermi energy, a similar conduction mechanism is expected for all Prussian blue analogs with transition-metal ions. Therefore if these materials are to be utilized as spin valves, the magnetic order must persist at temperatures where hopping conduction is feasible in addition to a simultaneous asymmetry in the up

and down spin conduction bands. An additional prospect to modify the conductivity is to substitute ions with larger wave functions, such as f electrons, that may provide a transition to a metallic state. Currently, we are investigating ways to stabilize electrochemical films in vacuum environments to continue the above studies with different levels of reductive and oxidative doping as well as methods to control the oxidation with external stimuli to act as a switch.

This work was supported by a Grant-in-Aid for Scientific Research on Innovative Areas (“Coordination Programming” Area 2107, Grant No. 22108530) from MEXT, Japan, and D.M.P. acknowledges support from the East Asia and Pacific Summer Institutes program of the National Science Foundation.

-
- ¹H. J. Buser, D. Schwarzenbach, W. Petter, and A. Ludi, *Inorg. Chem.* **16**, 2704 (1977).
- ²A. Ito, M. Suenaga, and K. Ono, *J. Chem. Phys.* **48**, 3597 (1968).
- ³P. Day, *Molecules into Materials: Case Studies in Materials Chemistry—Mixed Valency, Magnetism and Superconductivity* (World Scientific Publishing, Hackensack, NJ, 2007).
- ⁴M. Verdager and G. S. Girolami, *Magnetism: Molecules to Materials V* (Wiley-VCH, Weinheim, 2005) Chap. “Magnetic Prussian Blue Analogs.”
- ⁵D. Davidson and L. A. Welo, *J. Phys. Chem.* **32**, 1191 (1928).
- ⁶K. Itaya, I. Uchida, and V. D. Neff, *Accounts Chem. Res.* **19**, 162 (1986).
- ⁷M. K. Carpenter and R. S. Conell, *Appl. Phys. Lett.* **55**, 2245 (1989).
- ⁸M. K. Carpenter and R. S. Conell, *J. Electrochem. Soc.* **137**, 2464 (1990).
- ⁹A. Xidis and V. D. Neff, *J. Electrochem. Soc.* **138**, 3637 (1991).
- ¹⁰D. R. Rosseinsky, J. S. Tonge, J. Berthelot, and J. F. Cassidy, *J. Chem. Soc. Faraday Trans.* **83**, 231 (1987).
- ¹¹O. Sato, T. Kawakami, M. Kimura, S. Hishiya, S. Kubo, and Y. Einaga, *J. Am. Chem. Soc.* **126**, 13176 (2004).
- ¹²S.-i. Ohkoshi, K. Nakagawa, K. Tomono, K. Imoto, Y. Tsunobuchi, and H. Tokoro, *J. Am. Chem. Soc.* **132**, 6620 (2010).
- ¹³J. C. Wojdel, I. d. P. R. Moreira, S. T. Bromley, and F. Illas, *J. Chem. Phys.* **128**, 044713 (2008).
- ¹⁴J. C. Wojdel, I. d. P. R. Moreira, S. T. Bromley, and F. Illas, *J. Mater. Chem.* **19**, 2032 (2009).
- ¹⁵A. Kumar, S. M. Yusuf, and L. Keller, *Phys. Rev. B* **71**, 054414 (2005).
- ¹⁶J. F. De Wet and R. Rolle, *Z. Anorg. Allg. Chem.* **336**, 96 (1965).
- ¹⁷K. Tennakone and W. G. D. Dharmaratne, *J. Phys. C* **16**, 5633 (1983).
- ¹⁸H. Ibach and H. Lüth, *Solid-State Physics* (Springer, New York, 2002).
- ¹⁹N. F. Mott, *Philos. Mag.* **19**, 835 (1969).
- ²⁰P. Day, F. Herren, A. Ludi, H. U. Güdel, F. Hulliger, and D. Givord, *Helv. Chim. Acta* **63**, 148 (1980).
- ²¹A. Flambard, F. Köhler, and R. Lescouëzec, *Angew. Chemie Int. Ed.* **48**, 1673 (2009).
- ²²G. A. Landrum, *YAEHMOP (Yet Another Extended Hückel Molecular Orbital Package), Version 3.0* (Cornell University, Ithaca, New York, 2006).
- ²³E. Carmell and G. Fovles, *Valency and Molecular Structure* (Butterworth and Co. Ltd, London, 1977).